International Journal of Food Microbiology 364 (2022) 109519

Contents lists available at ScienceDirect

International Journal of Food Microbiology

journal homepage: www.elsevier.com/locate/ijfoodmicro

Predicting *B. cereus* growth and cereulide production in dairy mix

Nathália Buss da Silva [a,b], Mariem Ellouze [b], Katia Rouzeau-Szynalski [b], Nicholas Johnson [c], Marcel H. Zwietering [a], Heidy M.W. den Besten [a,*]

[a] Food Microbiology, Wageningen University & Research, Wageningen, the Netherlands
[b] Food Safety Microbiology, Institute of Food Safety and Analytical Sciences, Food Safety Research Department, Nestlé Research, Lausanne, Switzerland
[c] Food Safety Microbiology, Quality Management, Nestlé Nutrition Product Technology Centre Konolfingen, Konolfingen, Switzerland

ARTICLE INFO

Keywords:
Spore formers
Emetic toxin
Time to toxin
Modelling
Kinetics
Food safety

ABSTRACT

This study aims to quantify growth and cereulide production by *Bacillus cereus* and their potential correlation in an intermediate dairy wet-mix. Systematic experiments were carried out using the emetic reference strain F4810/72 in the suboptimal range of temperature of 12 °C to 20 °C. Growth and cereulide kinetic parameters were estimated and the three parameters (i) time to first cereulide quantification (t_{cer}), (ii) maximum specific growth rates (μ_{max}) and (iii) cereulide production rates (k) were modelled as a function of temperature. As temperature increased, growth lag time and t_{cer} were shorter while microbial increase and cereulide production happened earlier, and at higher rates. Maximum concentration of cells and maximum cereulide concentration proved to be temperature-independent, reaching the average values of 7.9 ± 0.3 $\log_{10}$(CFU/mL) and 2.6 ± 0.2 $\log_{10}$(ng.g^{-1}) respectively. Moreover, the time to reach the widely used threshold of 5 $\log_{10}$CFU/mL (t_{5log}) was tested against t_{cer}, and this suggested that this threshold can be used with increased confidence at lower temperatures to assure toxin is not quantified in this matrix. The average t_{cer} were equal to 314 h, 118 h, 73 h and 45 h for 12 °C, 15 °C, 18 °C and 20 °C respectively. A validation study was performed using independent data sets obtained with the same strain in other dairy matrices. The microbial growth models presented good predictive power even when extrapolated beyond the temperature range of construction. Nevertheless, the models proposed for prediction of toxin production over time presented limitations, especially for food matrices that deviate significantly from the original matrix for which the model was developed, making cereulide predictions less accurate. Our findings suggest that similar modelling approaches can be used to predict growth, time to first cereulide quantification as well as cereulide formation over time for a specific matrix, but that matrix-extrapolations are more suitable for growth than for cereulide.

1. Introduction

Bacillus cereus is a pathogenic bacterium commonly found in raw materials and processed foods (Ceuppens et al., 2011; Guo et al., 2021; Park et al., 2020; Wijnands et al., 2006). It is of particular concern for the food industry since its spores can endure high temperature short time (HTST) pasteurization, resist spray drying and survive in final products (McAuley et al., 2014). Spore-forming bacteria are ubiquitous in nature, and contamination has been shown to occur along the whole processing line (Eneroth et al., 2001), hence effective control of spore-forming bacteria in dairy products and processing environment is still challenging (Andersson et al., 1995; Huang et al., 2021; Oliveira Silva et al., 2018).

B. cereus can cause food poisoning through the production of either diarrheic enterotoxins or an emetic toxin, namely cereulide. While enterotoxins are formed in the gastrointestinal tract after contaminated food is consumed, cereulide is pre-formed in food matrices or ingredients by emetic strains of *B. cereus*. Due to the extreme heat and pH stability of cereulide, posterior processing can inactivate the microorganism but will not destroy cereulide. The emetic toxin is not inactivated by proteolytic enzymes in the gastrointestinal tract either (Agata et al., 1994; Delbrassinne et al., 2011; Shinagawa et al., 1996), which consequently can lead to intoxication.

Cereulide is a cyclic 1.2-kDa dodecadepsipeptide [D-O-Leu-D-Ala-L-O-Val-L-Val]$_3$ produced by a nonribosomal peptide synthetase, encoded by the 24-kb cereulide synthetase (*ces)* genecluster, which is located on a 208-kb pXO1-like megaplasmid (Ehling-Schulz et al., 2006). As a secondary metabolite, cereulide's formation mechanism is highly complex

* Corresponding author at: Food Microbiology, Wageningen University & Research, P.O. Box 17, 6700 AA Wageningen, the Netherlands.
E-mail address: heidy.denbesten@wur.nl (H.M.W. den Besten).

https://doi.org/10.1016/j.ijfoodmicro.2021.109519
Received 7 June 2021; Received in revised form 13 December 2021; Accepted 28 December 2021
Available online 3 January 2022

and, up to this point, not completely understood. In the same way that *B. cereus* strains are highly variable in terms of their growth limits (Carlin et al., 2013; EFSA, 2005; Guinebretière et al., 2008), some studies have suggested that cereulide production can also vary significantly depending on the strain and environmental conditions such as storage temperature and food matrix (Delbrassinne et al., 2011; Ellouze et al., 2021; Jääskeläinen et al., 2004; Rajkovic et al., 2006; Shaheen et al., 2006; Szabo et al., 1991). Moreover, the environmental conditions at which emetic toxin is produced differs from that for growth (Apetroaie-Constantin et al., 2008; Finlay et al., 2000; Häggblom et al., 2002; Rajkovic et al., 2006). For example, Rajkovic et al. (2006) observed that aeration of cultures had a negative effect on cereulide production, without affecting growth. Apetroaie-Constantin et al. (2008) observed that no cereulide was produced at temperatures of 41 °C or beyond, although the strains grew to temperatures of up to 48–50 °C.

Due to the lack of understanding on the correlation between *B. cereus* growth and cereulide production, currently available guidelines for control of this microorganism in food are purely based on cells concentration, established at maximum 10^5 CFU/g or mL (EFSA, 2005; EFSA, 2016). Literature has so far focused on the time cereulide starts being formed and some studies (Bursová et al., 2018; Rajkovic et al., 2006) have determined that cereulide is only formed at the end of exponential/beginning of stationary phase. But to date, no systematic analysis of kinetic data is available on cereulide production as function of time from the moment of inoculation until when *B. cereus* reaches the stationary phase. The enabling improvements in liquid chromatography - mass spectrometry technology for accuracy and sensitivity of toxin quantification in food matrices has made more informative modelling approaches possible, particularly closer to the point of toxin initiation.

In this paper we aim to fill this knowledge gap by quantifying the growth kinetics of *B. cereus* and cereulide production in an irradiated intermediate dairy wet mix (DWM) and proposing appropriate modelling approaches to identify first formation of toxin and its production along *B. cereus* growth. We also validate the predictions in similar dairy products to evaluate the prediction quality of the models. Our findings can be used in quantitative microbial risk assessments that evaluate the safety risk of foods contaminated with *B. cereus*.

2. Material and methods

2.1. Growth of B. cereus in dairy matrix

2.1.1. Preparation of stock culture

After streaking strain F4810/72 onto Trypticase Soy Agar with 0.6% Yeast Extract (TSAye) and incubating for 24 h at 37 °C to check for purity, one isolated colony was inoculated into BHI (Brain Heart Infusion) broth and incubated for 24 h at 37 °C. Then, 1 mL of the culture was added to 10 mL of sterile 80% glycerol and put into sterile 1 mL-tubes and stored at −80 °C.

2.1.2. Preparation of working culture

One tube of frozen stock culture was taken out and a superficially thawed layer was removed with a sterile loop and inoculated into 10 mL of BHI and incubated for 8 h at 30 °C. Subsequently, 100 μL of this primary culture was put into 9.9 mL of BHI and incubated for 18 h at 30 °C to have a standardized working culture.

2.1.3. Matrix

One batch of intermediate dairy wet-mix (DWM) (see basic components and physical-chemical characteristics in Table 1) was sent for irradiation at 10 kGy (Steris, Netherlands) in several 500 mL bottles and kept at −20 °C. Before the beginning of the experiments of each of the three replicates, two irradiated bottles were set aside in the fridge overnight. The temperature of the matrix was equilibrated by placing the bottles in the respective temperature-set incubators for at least half an hour before inoculation to ensure that the matrix temperature was equivalent to the test-temperature (the equilibration time was verified in a pre-experiment and was found to be below 30 min). The matrix "intermediate mix" refers to storage between initial heat treatment and the final heat treatment of the production process.

Table 1
Physical-chemical characteristics and components of DWM used in this study

Characteristic/Components	Value
Water activity	0.98
pH	6.8
Total solids (%)	33.1%
Fat (*w*/w solids)	23.9%
Protein (w/w solids)	12.5%
Carbohydrates (w/w solids)	56.8%
Minerals (w/w solids)	2.4%

2.1.4. Samples inoculation and growth quantification

The working culture was decimally diluted in BHI and added (0.67% v/v) to 150 mL of matrix targeting an initial concentration of ~2 $\log_{10}$ CFU/mL. For *B. cereus* quantification, selective medium plates (Bacara, bioMérieux) were used. The effect of temperature on *B. cereus* growth was studied by incubating inoculated bottles of irradiated matrix with F4810/72 strain at four different temperatures: 12 °C, 15 °C, 18 °C, and 20 °C, simulating different conditions at which this intermediate matrix would be stored before being further processed during normal operating conditions or occasional temperature abuses. Carlin et al. (2013) have determined cardinal values for the F4810/72 strain: T_{min} has been reported to be equal to 7.9 °C and T_{opt} equal to 38.7 °C, meaning that the evaluated interval is within suboptimal temperature range for growth. Samples were taken at different time points for the studied temperatures to cover the whole growth range. Three biologically independent replicates were performed for each temperature.

2.2. Cereulide measurement

Cereulide samples were taken by filling two Eppendorf tubes with 2 mL from each of the inoculated bottles that were also used to quantify the growth of *B. cereus*. Samples were then immediately frozen in liquid nitrogen for further cereulide extraction. Sampling times for cereulide and *B. cereus* quantification varied with the temperature of incubation and were independent of each other.

2.2.1. Cereulide extraction

Cereulide was extracted as described in the ISO 18465-2017. Briefly, previously frozen samples were thawed in the fridge (4 °C) and then homogenized by mixing prior to extraction. Samples were kept on ice during the weighing and the addition of the internal standard and acetonitrile. For that, 1 g (± 0.01 g) of homogenized sample was weighted into a 15 mL Falcon tube and then spiked with 1 mL of $^{13}C_6$-cereulide 15 ng/mL solution (ISTD, internal standard) (Chiralix, Nijmegen, The Netherlands) and 9 mL of acetonitrile (Honeywell Riedel-de Haën, Charlotte, USA) was added. Tubes were checked to guarantee they were hermetically closed and mixed. The tubes of extract were placed in the orbital shaker (VXR basic Vibrax; IKA, Staufen, Germany) and shaken for at least 60 min at 1800 rpm. The extracts were then centrifuged and 2 mL of supernatant was filtered into an amber glass vial.

2.2.2. Cereulide quantification

In order to quantify the cereulide concentration, the extracted components were isocratically separated using Ultra High Performance Liquid Chromatography (UPLC) and detected using tandem mass spectrometry. Quantification was done using an external calibration curve with standard (synthesized) cereulide (Chiralix, Nijmegen, The Netherlands) concentrations varying from 0.01 ng/g to 100 ng/g and fixed ISTD concentrations (1.5 ng/g). Cereulide concentrations were

expressed in ng/g of matrix.

For cereulide quantification, UPLC-ESI-TOF MS analysis was carried out using Waters Acquity HClass Bio UPLC system with Synapt G2Si HDMS (Waters, Milford, MA, USA) with an electrospray interface (ESI). The chromatograph system was equipped with an Acquity UPLC BEH C18 column (1.7 µm, 2.1 mm × 50 mm). The column and auto sampler temperature were set on 30 °C and 12 °C respectively and flow rate was set to 0.5 mL/min. The mobile phase consisted of eluent A (water/(ACN and MeOH (80:20, v/v)) 95:5, v/v) and eluent B (ACN and MeOH (80:20, v/v))/ water, 98:2, v/v). Both eluents contained 0.3% formic acid and 1 mM ammonium acetate. The elution program for gradient is eluent B at 70% and eluent A at 30%.

All analyses were performed with lock mass correction using leucine enkephalin (Tyr-Gly-Gly-Phe-Leu, m/z 556.2771), in a solution (150 pmol/µL) of 50:50 water: acetonitrile. Calibration of the Synapt G2-Si in the range from m/z 40 to 1200 was performed using a solution of sodium iodate (5 mmol/L) in 2-propanol/H_2O (9:1, v/v). The method was based on the ISO 18465 2017–01, modified to lower its quantification limit.

The data was collected and processed by MassLynx software v. 4.1. The calibration and quantification of cereulide and ISTD concentration were carried out by TOF MS2 spectra integration TIC spectra of the MS/MS 1171 and 1176 daughter ions, being $m/z = 172.15$ the quantifier ion for ISTD and m/z = 357.25 the quantifier ion for cereulide. Limit of Detection (LoD) and Limit of Quantification (LoQ) are 0.01 ng/g and 0.02 ng/g of extract, respectively, and translates into LoD and LoQ of 0.1 ng/g and 0.2 ng/g of matrix, respectively. When samples were concentrated, LoQ and LoD were ten times lower. The method with lower detection and quantification limits (for samples that went through the concentration step) is described in detail in Ellouze et al. (2021).

2.3. Modelling of B. cereus growth

In order to estimate the growth parameters, the adapted model of Baranyi and Roberts (1994) with m = 1 and $\nu = \mu_{max}$, presented in Eq. (2.1), was fitted to the obtained log counts by using the Excel add in DMFit (version 3.5, kindly provided by ComBase).

$$log_{10}N(t) = log_{10}N_0 + \frac{\mu_{max}}{ln(10)}A(t) - \frac{1}{ln(10)}ln\left(1 + \frac{e^{\mu_{max}A(t)} - 1}{10^{(log_{10}N_{max} - log_{10}N_0)}}\right) \quad (2.1)$$

$$\text{with}: A(t) = t + \frac{1}{\mu_{max}}ln\left[e^{-\mu_{max}t} + e^{-\mu_{max}\lambda} - e^{-\mu_{max}t-\mu_{max}\lambda}\right]$$

where μ_{max} is the maximum specific growth rate in 1/h, λ is lag duration in hours, $\log_{10}N_0$ is the initial population in $\log_{10}$ CFU/mL and $\log_{10}N_{max}$ the maximum population reached in $\log_{10}$ CFU/mL.

When an initial decrease in the counts was observed, values below $\log_{10}N_0$ were considered as part of the lag phase.

The goodness of fit was evaluated by means of the standard error of the regression (se(fit)) presented in Eq. (2.2).

$$se(fit) = \sqrt{\sum_{i=1}^{n}\frac{(y_i - f_i)^2}{n - p}} \quad (2.2)$$

where y_i are observations, f_i are the fitted values, n is number of observations and p is the number of parameters in the model.

By means of the growth parameters and Eq. (2.1), the time taken for *B. cereus* to reach 5 $\log_{10}$CFU/mL (t_{5log}) could be estimated for each of the replicates.

The effect of temperature on μ_{max} was assessed by fitting the Ratkowsky et al. (1982) model (Eq. (2.3)) to the square root of the μ_{max} estimates.

$$\sqrt{\mu_{max}} = b(T - T_{min}) \quad (2.3)$$

where T is temperature [°C], b is the slope [1/(√h .°C)] and T_{min} is the theoretical minimum temperature for growth [°C]. Model 95% prediction interval was determined considering the regression ±1.96 times the standard error of prediction (Eq. (2.2)).

2.4. Modelling of cereulide production

The same primary model (Baranyi and Roberts (1994)) (Eq. (2.1)) used for describing *B. cereus* growth was used and adapted to describe cereulide production over time (see Eq. (2.4)), due to its sigmoid shape of the $\log_{10}$ transformed cereulide concentration.

$$log_{10}C(t) = log_{10}C_0 + \frac{k}{ln(10)}B(t) - \frac{1}{ln(10)}ln\left(1 + \frac{e^{kB(t)} - 1}{10^{(log_{10}C_{max} - log_{10}C_0)}}\right) \quad (2.4)$$

$$\text{with}: B(t) = t + \frac{1}{k}ln\left[e^{-kt} + e^{-k\lambda_{cer}} - e^{-kt-k\lambda_{cer}}\right]$$

where k is the specific cereulide production rate in ln(ng/g)/h, λ_{cer} is the cereulide lag time in hours, $\log_{10}C_0$ is the initial cereulide level in $\log_{10}$ ng/g and $\log_{10}C_{max}$ is the maximum cereulide level reached in $\log_{10}$ ng/g. k was evaluated and visualized in the $\log_{10}$ scale ($\log_{10}$(ng/g)/h), by dividing the results of each fitting by 2.303.

The goodness of fit was evaluated by means of the standard error of the regression (se(fit)) presented in Eq. (2.2).

The effect of temperature on the cereulide production rates was assessed by adapting and fitting the Ratkowsky et al. (1982) model (Eq. (2.5)) to the results obtained from the primary fitting.

$$\sqrt{k} = d(T - T_{min.cer}) \quad (2.5)$$

where T is temperature [°C], d is the slope [$\sqrt{(\log_{10}(ng/g)/h)}$.1/°C)] and $T_{min.cer}$ is the theoretical minimum temperature for cereulide production [°C]. Model 95% prediction interval was determined considering the regression ±1.96 times the standard error of prediction (Eq. (2.2)).

The precise estimation of cereulide lag times (λ_{cer}) was compromised by the difficulty to pro-actively identify adequate sampling times capturing the start of production and describing the cereulide kinetic during exponential production. Taking this and data uncertainty into account, a complementary approach was used to estimate t_{cer} (in h), the time taken for cereulide to be produced, namely the time to first quantification. The t_{cer} was estimated by a linear interpolation between the last sampling point where cereulide levels were below $\log_{10}$(LoQ) level and the subsequent point where cereulide was quantified (Point A and B) in Fig. 1. The interpolation method was proposed by Hornung and Reed (1990) and has already been successfully used for t_{cer} estimation in

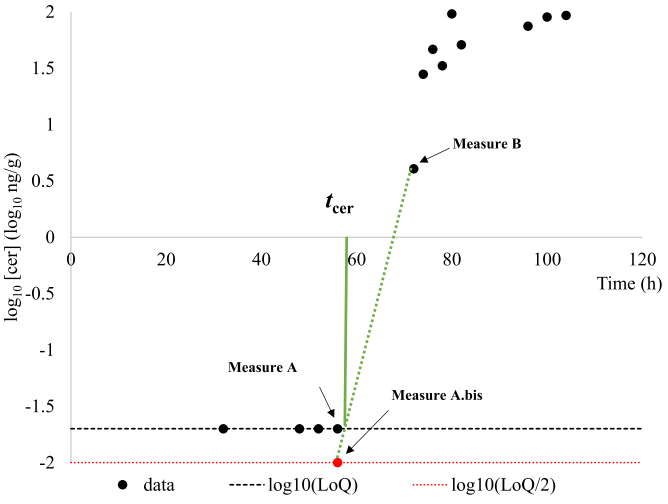

Fig. 1. Linear interpolation to calculate t_{cer}, the time to quantifiable cereulide level.

different matrices by Ellouze et al. (2021). The $\log_{10}$(LoQ/2) value was assigned to the last time point when the measured cereulide concentration was below LoQ level (a point called A.bis in Fig. 1). Then the slope and intercept of the line combining A.bis and B were used to estimate t_{cer}:

$$t_{cer} = \frac{log_{10}LoQ - intercept}{slope} \quad (2.6)$$

Three approaches were evaluated to predict cereulide formation: (*i*) prediction of the time to first cereulide formation t_{cer} using t_{5log}, (*ii*) prediction of t_{cer} using a model for dependence of t_{cer} with temperature, and (*iii*) prediction of cereulide production over time considering cereulide formation rate (k) and t_{cer}, using the three-phase linear model (Eqs. (2.7a) and (2.7b)), adapted from Buchanan et al. (1997).

$$log_{10}C(t) = log_{10}(LoQ) \text{ for } t \leq t_{cer} \quad (2.7a)$$

$$log_{10}C(t) = min(log_{10}C_0 + k(t - t_{cer}), log_{10}C_{max}) \text{ for } t > t_{cer} \quad (2.7b)$$

2.5. Validation

In order to evaluate the applicability and extendibility of the modelling approaches adopted here, a validation study was carried out with data for growth and cereulide formation by the same strain (F4810/72) in five other matrices: (1) non-irradiated intermediate dairy wet-mix, same matrix used for models construction without going through pre-irradiation process (non-irradiated DWM), (2) irradiated intermediate dairy wet-mix with total solids content of 30% (DWM30), (3) irradiated intermediate dairy wet-mix with total solids content of 35% (DWM35), (4) irradiated intermediate dairy wet-mix with total solids content of 40% (DWM40), and (5) reconstituted dairy-based matrix (RDM). The first matrix was chosen to verify whether naturally present background flora can interfere in growth or cereulide production. The second (DWM30) to verify whether growth and cereulide production are similar in matrices of the same kind, while the other three matrices were selected to assess whether changes in the original matrix (either formulation or moisture content) can have a significant role in *B. cereus* growth and/or cereulide production.

The root mean square error (Eq. (2.8)) was selected to evaluate prediction performance.

$$RMSE = \sqrt{\sum_{i=1}^{n} \frac{(\hat{y}_i - y_i)^2}{n}} \quad (2.8)$$

where $\hat{y}_i$ are predicted values, y_i are observed data and n are the number of observations.

3. Results

3.1. Bacillus cereus growth

Growth of *B. cereus* was observed at all tested temperatures, confirming the suboptimal temperature region of mesophilic *B. cereus* strains with the higher maximum specific growth rate at the higher temperature (Table 2).

The square-root plot following the Ratkowsky et al. (1982) model is shown in Fig. 2, with its parameters b equal to 0.044 ± 0.003 $h^{-1/2}$ °C^{-1} and T_{min} equal to 4.98 ± 0.32 °C.

3.2. Modelling cereulide formation

Cereulide was quantified in DWM at all studied temperatures (Fig. 3A). Variability among replicates appears more pronounced at 18 °C, while remaining fairly small for 20 °C, 15 °C and 12 °C. Regarding the variability between temperatures, 12 °C is easily distinguished with cereulide being produced later and at lower rate, followed by 15 °C, while data at 18 °C and 20 °C are quite close to each other for some of the replicates.

Two modelling approaches were considered here: (*i*) with the objective of estimating the time to first cereulide formation with t_{5log}

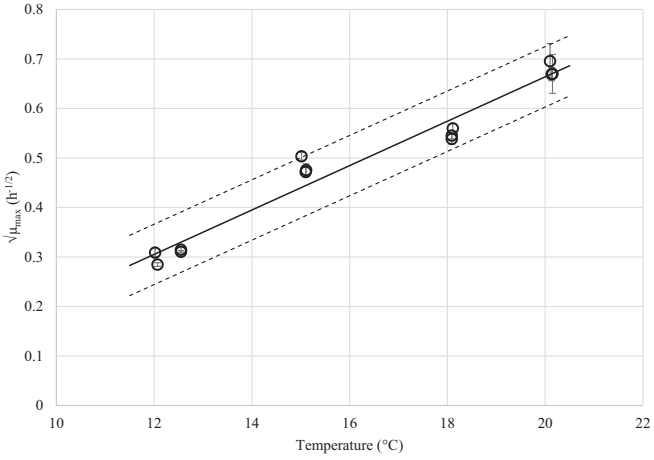

Fig. 2. Secondary modelling using Ratkowsky model for the effect of temperature on maximum specific growth rates of F4810/72 strain when growing in DWM. Open circles are the raw data, continuous line is the fitted model to the respective data, error bars represent standard error of estimated maximum specific growth rates and the dashed lines represent the model prediction interval at 95% level.

Table 2
Primary parameters estimates with their respective standard errors, and quality of fitting parameter se(fit) for the growth of *B. cereus* F4810/72 in irradiated dairy intermediate wet-mix (DWM)

T (°C)	T_{real} [b] (°C)	Replicate	μ_{max} (1/h) [se]	λ (h) [se]	$\log_{10}N_0$ ($\log_{10}$ CFU/mL)	$\log_{10}N_{max}$ ($\log_{10}$ CFU/mL) [se]	se(fit)
12	12.0 ± 0.1	A	0.095[0.008]	260.8[16.4]	2.52	7.19[0.17]	0.2602
12	12.1 ± 0.2	B	0.081[0.004]	103.5[13.0]	2.36	*nd*[a]	0.2611
12	12.6 ± 0.1	C	0.099[0.005]	118.7[11.9]	2.26	7.45[0.15]	0.2702
15	15.1 ± 0.1	A	0.222[0.010]	73.9[4.4]	2.55	7.98[0.10]	0.1854
15	15.0 ± 0.1	B	0.253[0.008]	53.5[2.9]	2.19	7.82[0.12]	0.1567
15	15.1 ± 0.1	C	0.226[0.013]	51.4[5.2]	2.30	7.81[0.10]	0.2301
18	18.1 ± 0.0	A	0.313[0.009]	24.4[1.8]	2.37	7.99[0.05]	0.0925
18	18.1 ± 0.1	B	0.290[0.011]	24.2[2.7]	2.26	8.00[0.07]	0.1496
18	18.1 ± 0.1	C	0.297[0.007]	25.3[1.7]	2.21	8.00[0.05]	0.0976
20	20.2 ± 0.2	A	0.449[0.039]	28.0[3.9]	2.52	8.16[0.08]	0.2033
20	20.1 ± 0.2	B	0.484[0.035]	33.0[3.4]	2.54	8.30[0.07]	0.1803
20	20.1 ± 0.1	C	0.448[0.013]	24.5[1.8]	2.17	8.04[0.08]	0.1573

[a] nd = not determined.
[b] T_{real} stands for the measured temperature inside the incubator. Average and standard deviations are presented.

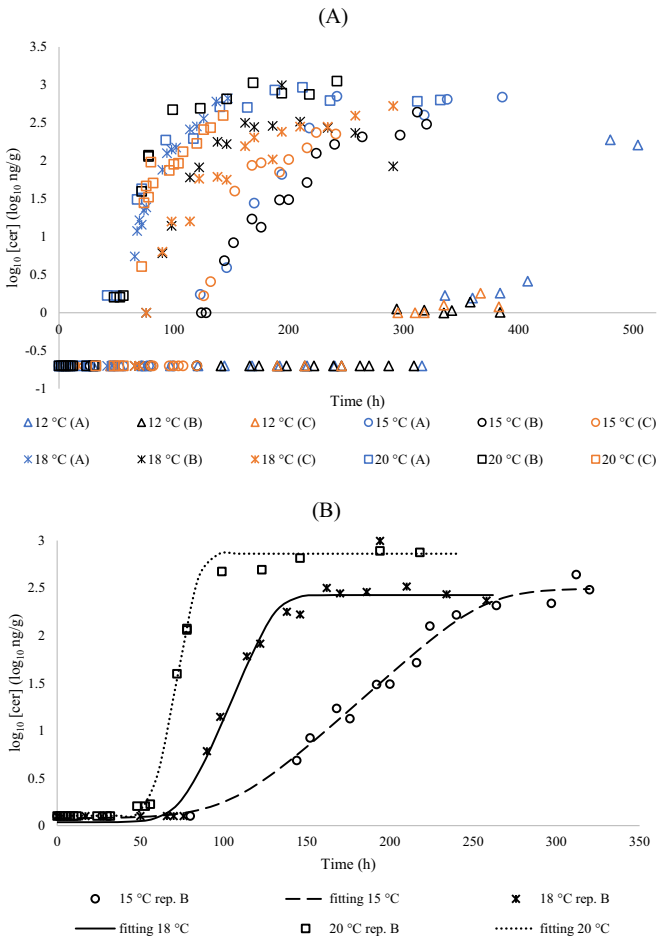

Fig. 3. (A) Logarithm of cereulide concentration vs. time for the four tested temperatures in DWM. Symbols represent different temperatures: 12 °C (triangles), 15 °C (circles), 18 °C (stars) and 20 °C (squares) with replicate A in blue, replicate B in black and replicate C in orange. (B) Example of fitting of Baranyi and Roberts (1994) model to cereulide production data at 15 °C (circles), 18 °C (stars) and 20 °C (squares). (For interpretation of the references to colour in this figure legend, the reader is referred to the web version of this article.)

and t_{cer} and (*ii*) to evaluate cereulide production over time with cereulide formation rate (k). The time to first quantification of cereulide (t_{cer}) was estimated for each of the replicates in irradiated DWM (Table 3). In Fig. 3B, three of the fittings performed to obtain cereulide primary parameters are presented and the fitting results for all replicates are presented in Table 3.

As temperature increased, t_{cer} decreased, suggesting a correlation between temperature and first cereulide formation. Therefore, the square-root link-function was applied here to the reciprocal of t_{cer} parameter (a "rate-like" quantity) as suggested by Ellouze et al. (2021). Fig. 4 shows a strong correlation (p-value = 0.0056) between the square root of t_{cer} reciprocal and temperature. The relevance of this approach to predict the time to first quantification was assessed in the validation study.

Current guidelines for control of *B. cereus* in food products relies upon bacterial concentration. Therefore, we assessed the safety of this measure for control of toxin in food by evaluating whether cereulide could be quantified (i.e. equal or higher than LoQ) only after *B. cereus* concentration reaches a 5 $\log_{10}$CFU/mL threshold. The estimated t_{5log} values are shown in Table 3 and were estimated based on the fitted primary growth model (results presented in Table 2). Fig. 5 correlates the time to reach 5 $\log_{10}$CFU/mL (t_{5log}) with the estimated time to first

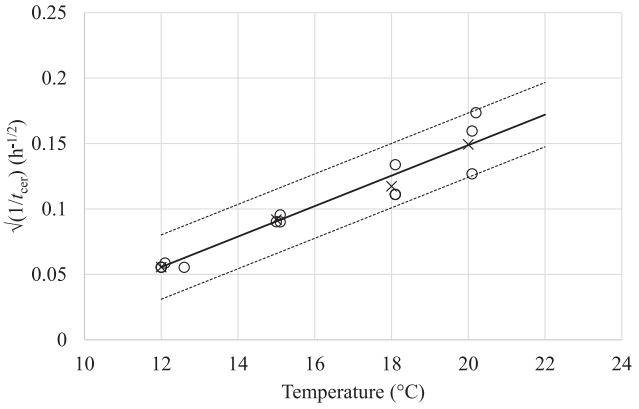

Fig. 4. Square-root of reciprocal of estimated time to first quantification of cereulide (t_{cer}) vs. temperature for DWM. Open circles are the raw data, crosses are averages per temperature, continuous line is the fitted model, and the dashed lines represent the model prediction interval at 95% level.

Table 3
Times to first quantification of cereulide (t_{cer}), times at which *B. cereus* concentration reaches 5 $\log_{10}$ CFU/mL (t_{5log}), and values of estimated primary parameters for cereulide with their respective standard errors and quality of fitting parameter for DWM at different temperatures and replicates

		Approach (i)		*Approach (ii)*			
T (°C)	Rep.	t_{cer} (h)[c]	t_{5log} (h)	k ($\log_{10}$ (ng/g)/h) [se]	$\log_{10}C_{max}$ ($\log_{10}$ (ng/g)) [se]	λ_{cer} (h) [se]	se (fit)
12	A	325.0	324.0	*nd*[a]	*>2.00*[b]	*>250*[b]	*nd*[a]
12	B	290.4	188.6	*nd*[a]	*>0.14*[b]	*>250*[b]	*nd*[a]
12	C	326.1	188.4	*nd*[a]	*>0.26*[b]	*>250*[b]	*nd*[a]
12	*Av.[sd]=*	*313.8[20.3]*	*233.7[78.2]*	*nd*[a]	*nd*[a]	*nd*[a]	*nd*[a]
15	A	109.7	105.0	0.027 [0.002]	2.78 [0.04]	126.50 [4.32]	0.0768
15	B	123.1	82.0	0.016 [0.001]	2.49 [0.06]	103.50 [9.75]	0.1063
15	C	122.7	80.8	0.019 [0.002]	*nd*[a]	96.21 [18.33]	0.3093
15	*Av.[sd]=*	*118.5[7.6]*	*89.2[13.6]*				
18	A	55.8	46.4	0.041 [0.004]	2.65 [0.07]	42.65 [5.14]	0.1393
18	B	81.0	48.0	0.042 [0.009]	2.43 [0.07]	74.23 [8.88]	0.2128
18	C	81.0	48.6	0.023 [0.004]	2.46 [0.09]	58.54 [13.34]	0.2151
18	*Av.[sd]=*	*72.6[14.5]*	*47.7[1.1]*				
20	A	33.2	40.8	0.049 [0.009]	2.75 [0.06]	42.94 [6.27]	0.1743
20	B	39.3	44.8	0.094 [0.012]	2.86 [0.03]	56.83 [2.39]	0.08709
20	C	62.1	39.0	0.116 [0.038]	2.19 [0.08]	64.58 [4.13]	0.2403
20	*Av.[sd]=*	*44.9[15.3]*	*41.5[2.9]*				

[a] nd = not determined; at 12 °C, no fitting was performed due to limited data.
[b] Estimated value based on data since fitting was not possible at 12 °C.
[c] t_{cer} was estimated through linear interpolation considering LoQ equal to 0.02 ng/g (see Fig. 1).

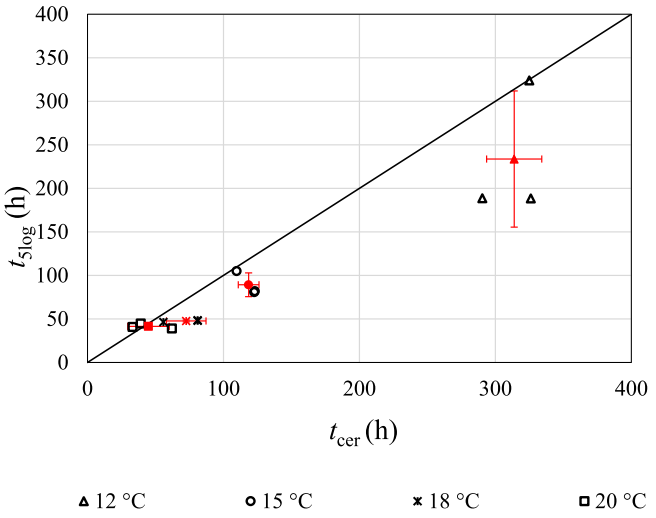

Fig. 5. Time to reach 5 $\log_{10}$ CFU/mL (t_{5log}) versus time to first quantification of cereulide (t_{cer}) in DWM when inoculum level is ~2 $\log_{10}$ CFU/mL. Replicates are represented in open black symbols and averages per temperature in filled red symbols. (For interpretation of the references to colour in this figure legend, the reader is referred to the web version of this article.)

cereulide quantification (t_{cer}) for all replicates in irradiated dairy mix at the tested temperatures. For temperatures below or equal to 18 °C, all data were below the equivalence line where t_{cer} is higher than t_{5log}, while for two replicates at 20 °C the time to first quantification of cereulide was slightly shorter than time for *B. cereus* to reach the specified threshold (33.2 h and 39.3 h compared to 40.8 h and 44.8 h). However, t_{cer} is always higher than t_{5log} if we take the averages per temperature. Seemingly, the difference between the times represented in Fig. 5 increases as temperature decreases, noted by the closeness of data at 15 °C, 18 °C and 20 °C to the equivalence line, suggesting that the lower is the temperature, the higher are the *B. cereus* counts at t_{cer} in this matrix. Note that the LoQ that is used as threshold to estimate t_{cer} is equipment dependent. In the present study, LoQ is equal to 0.02 ng/g, but higher values have been reported in the literature: Häggblom et al. (2002) reported an LoQ equal to 1 ng/g, Agata et al. (2002) equal to 5 ng/g and Guerin et al. (2017) an LoQ of 0.33 ng/g. Assessing t_{cer} with higher LoQs would result in an overestimation of this parameter. Moreover, the estimated t_{cer} values were valid for an inoculum level of 2–2.5 $\log_{10}$CFU/mL, which represented a rather highly contaminated matrix. The literature reports much lower numbers (−1 to 0 $\log_{10}$CFU/mL) for natural contamination of milk with *B. cereus* (Bartoszewicz et al., 2008; Svensson et al., 2004; Svensson et al., 2006).

Among the tested conditions in DWM, 12 °C is the temperature at which *B. cereus* F4810/72 grows and produces cereulide later and seemingly at slowest rate. However, 12 °C is also the condition with more erratic cereulide production data, preventing an estimation of the primary parameters (due to lack of convergence during fitting).

The maximum cereulide concentration ($y_{max.cer}$) reached for the performed kinetic experiments remained fairly constant (for all temperatures, $\overline{y_{max.cer}}$ [sd] = 2.58 [0.22] $\log_{10}$ (ng.g^{-1})) and is therefore independent of temperature at 95% significance level (p-value = 0.873).

Fig. 6 presents the relationship between square-root of cereulide production rates (k) and temperature. Even though the observed variability is quite high, the cereulide production rate (k) is positively correlated to temperature in the range 15 °C -20 °C (p-value = 0.048) at 95% confidence level.

3.3. Validation

A validation study was carried out using five matrices: non-irradiated DWM, reconstituted dairy-based matrix (RDM), intermediate dairy wet-mix with total solids content of 30% (DWM30), of 35% (DWM35) and of 40% (DWM40).

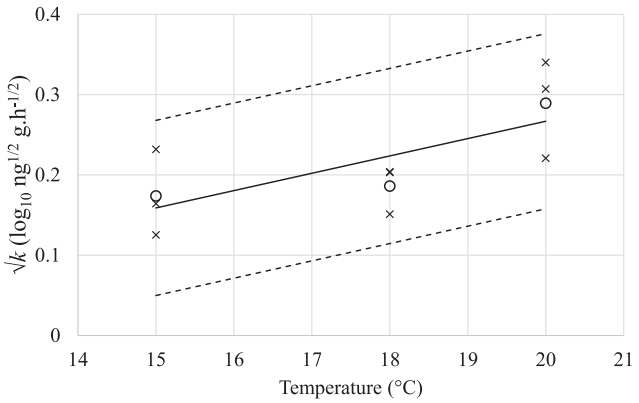

Fig. 6. Ratkowsky et al. (1982) secondary model describing dependence of square-root of cereulide production rates with temperature. Replicates are represented by crosses and averages per temperature are circles. Continuous line is fitted model and dashed lines represent 95% prediction interval.

Fig. 7 compares the maximum specific growth rates obtained in the validation media with the model based on dairy wet-mix (total solids content of 33%) presented in Fig. 2. As data from temperatures above 20 °C were collected for RDM, the model was extrapolated from 20 °C to 31 °C, which is a reasonable extrapolation since the square-root of the growth rates follow a linear relationship with temperature in the sub-optimal growth region (Ratkowsky et al., 1982) and the optimal temperature for growth of this strain is 38.7 °C (Carlin et al., 2013). The calculated RMSE was 0.017 for non-irradiated DWM, 0.076 for RDM data and 0.105 for DWM at various total solids content, showing good agreement between the model developed in dairy wet-mix and the data observed in other similar matrices and suggesting matrix-extrapolation is possible for maximum specific growth rate prediction.

No cereulide was detected in non-irradiated DWM up to 24 days at 12 °C and detected only after 13 days (<0.02 ng/g) at 15 °C. Limited toxin formation was observed in the non-irradiated matrix, even at 18 °C and 20 °C where cereulide reached a maximum concentration of 0.4 and 1.3 ng/g, respectively, indicating that non-irradiated matrix supported about 1000 times less cereulide than the irradiated matrix. Therefore,

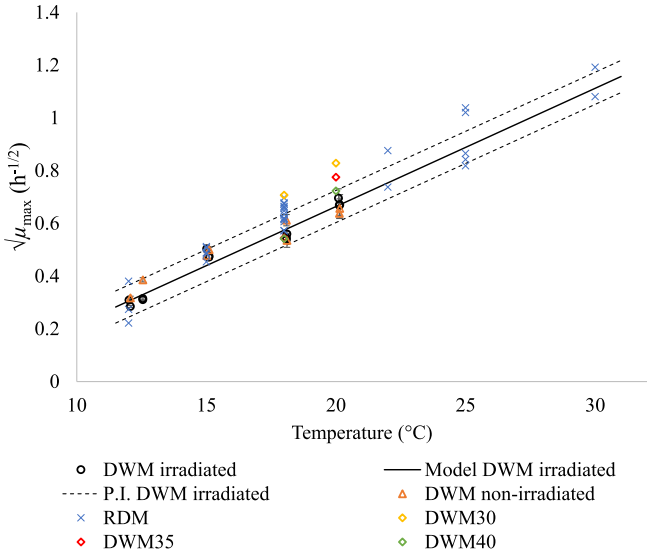

Fig. 7. Ratkowsky et al. (1982) model for specific growth rates of *B. cereus* F4810/72 built with dairy wet-mix (DWM) data (extrapolated version of model and P.I. presented in Fig. 2) and validation data in five other dairy matrices.

toxin modelling approaches were validated on the other four irradiated matrices. Non-irradiated DWM data can be found in the Supplementary material.

For cereulide, the validation was conducted using two approaches: (*i*) the times for first toxin quantification at various temperatures for the four matrices were compared to the data and secondary model presented in Fig. 4 and (*ii*) the predictions for cereulide production over time were generated (considering models and assumptions presented in Figs. 4 and 6) and compared to cereulide data in a similar dairy-based matrix with different TS contents (DWM30, DWM35 and DWM40) at 18 °C and 20 °C.

The first approach compares t_{cer} in the different matrices with the model developed in dairy wet-mix (Fig. 8) and one can observe that as temperature increases from 15 °C, the bigger is the discrepancy between the model and data in RDM. The same figure also shows that data for the three kinds of DWM were close to the upper boundary of the 95% prediction interval. That means the t_{cer} in dairy-based matrices with different TS are close to the expected range, while cereulide was quantified earlier in RDM than predicted for DWM. This suggested that the starting point of cereulide quantification is matrix dependent and that limited extrapolations to other type of matrices can be made when predicting t_{cer}. Even though the results are very similar for the different kinds of DWM, one can notice that the higher the total solids content, the lower is the maximum specific growth rate and the later cereulide is first quantified.

As for the validation of cereulide production over time, mean predictions were generated and plotted against data in the DWM adjusted for three different levels of total solids (DWM30, DWM35 and DWM40) as shown in Fig. 9 with the respective RMSE values for each individual set of data presented in Table 4. The maximum cereulide concentration reached was set to the observed mean value of 2.58 $\log_{10}$ ng/g and t_{cer} was considered as the time to first cereulide quantification.

In general, good agreement between predictions and the independent data were observed. As TS level increased, RMSE values also increased and a greater discrepancy between prediction and observations could be perceived. As predictions were based in the original dairy wet-mix with total solids content of 33%, this is not an unanticipated observation.

4. Discussion

In our study, the time to first quantification of cereulide (t_{cer}) could be estimated in irradiated dairy mix and, as suggested by Ellouze et al. (2021) when studying cereulide formation in a wide range of food

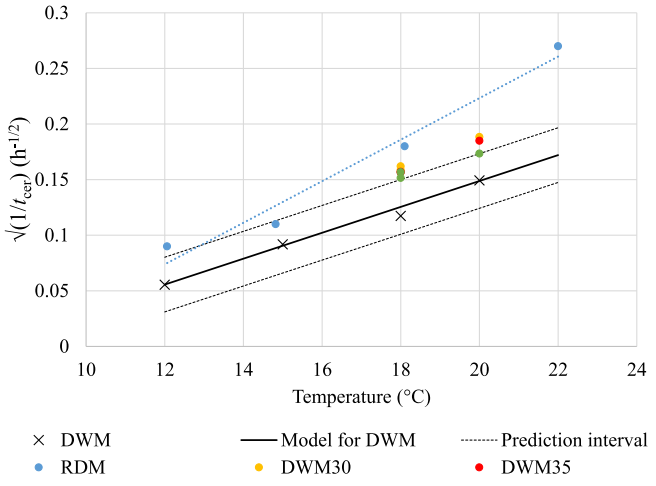

Fig. 8. Validation of model for first time to cereulide quantification developed with DWM data (black symbols and lines) compared to data in other dairy-based matrices (colored circles).

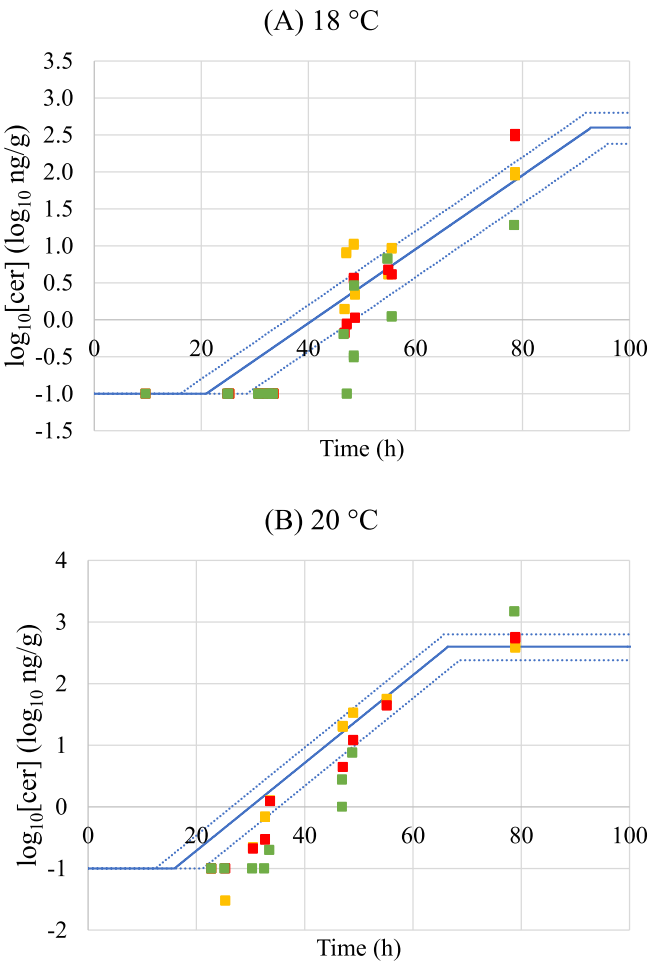

Fig. 9. Validation of cereulide production over time for three dairy wet-mixes (DWM) with different total solids content at 18 °C (A) and 20 °C (B). Continuous line represents prediction generated using modelling approaches developed for DWM along this study; dashed line represents the prediction interval at 95% confidence, squares are independent data for DWM30 (in yellow), DWM35 (in red) and DWM40 (in green). (For interpretation of the references to colour in this figure legend, the reader is referred to the web version of this article.)

Table 4
RMSE values for predictions of cereulide production over time when compared to data in intermediate dairy wet-mixes (DWM) at various total solids (TS) levels at 18 °C and 20 °C

T (°C)	TS (%)	RMSE
18	30	0.430
18	35	0.558
18	40	0.632
20	30	0.460
20	35	0.469
20	40	0.800

matrices, the square root of the reciprocal of t_{cer} follows a linear relationship with temperature. This serves as a valuable tool to predict maximum storage times for DWM at temperatures ranging from 12 °C to 20 °C.

When comparing *B. cereus* growth and cereulide production in irradiated and non-irradiated DWM, we observed that cereulide production was suppressed by the presence of background flora in the non-irradiated matrix. This agrees with Rajkovic et al. (2006), who observed the same when evaluating toxin production in a variety of matrices. However, no differences were observed between *B. cereus*

growth rates of non-irradiated and irradiated matrices in the present study. This confirms the dissimilarities between growth and toxin formation and highlights the need for the simultaneous measurement of *B. cereus* growth and cereulide production.

Shaheen et al. (2006) observed that diluting the reconstituted food with water resulted in increased toxin production when evaluating cereulide production in different infant formulae. This trend was not observed here for our validation matrix (DWM) at three different total solids (TS) content. The measured concentrations were rather comparable for the temperatures of 18 °C and 20 °C, possibly due to the fact that TS levels varied from 30% to 40% only. Walser et al. (2021) have investigated cereulide production in cow milk with various fat contents and have concluded that the emetic toxic has a clear affinity towards the lipid phase. This can explain the dissimilarities we have observed in the present study when evaluating cereulide production in various dairy-based matrices.

Similarly to growth, cereulide is produced earlier and at higher rate as temperature increases from 12 °C to 20 °C. In agreement, Guérin et al. 2017 observed that cereulide production by *Bacillus weihenstephanensis* BtB2–4 in agar media was 5 times higher when temperature increased from 8 °C to 10 °C or 15 °C and more than 100 times greater when the temperature went from 15 °C to 25 °C. Agata et al. (2002) studied the growth of *B. cereus* NC7401 in boiled rice and reported that cereulide production in a fixed time interval was higher when temperature increased from 20 to 35 °C.

Cereulide formation kinetics follows a sigmoid shape in the $\log_{10}$ scale. Its production does not start and evolves along with growth unlike some primary metabolites, such as lactic acid. Cereulide was detected only at late exponential phase in DWM when *B. cereus* counts were already above 5 $\log_{10}$ CFU/mL threshold and continues along the stationary phase for the temperatures of 12 °C, 15 °C and 18 °C, while cereulide was sometimes quantified just before or just after that *B. cereus* reached 5 $\log_{10}$ CFU/mL at 20 °C (Fig. 5). Similarly, Rajkovic et al. (2006) analysed cereulide formation in five different groups of commercial ready-to-eat food products and showed that for none of the products and temperature tested (12 °C, 22 °C and 28 °C) cereulide was detected (detection limit not reported) below 5 $\log_{10}$ CFU/g threshold. However, in contrary to this present study findings, Rajkovic et al. (2006) showed that *B. cereus* counts at cereulide detection times were higher for lower temperatures when compared with higher temperatures.

The t_{cer} coincided with t_{5log} at higher temperatures (18 °C and 20 °C), while t_{5log} is a fail-safe assumption for lower temperatures (15 °C and 12 °C) in the evaluated matrix. As one can easily determine t_{5log} based on bacterial counts without further testing for cereulide production, this threshold can be safely used as an indicator of cereulide concentrations below LoQ for closely related matrices. To the best of our knowledge, dose-response data are limited and have been obtained by semi-quantitative or indirect methods like vacuolation by the Hep-2 cell test (Finlay et al., 1999) or inhibition of sperm motility as described by Andersson et al. (2004). The minimum concentration of cereulide causing emetic food poisoning is still unknown and can be lower than the concentrations linked to outbreaks. Therefore, safety limits linked to cereulide consumption cannot be established without further investigation. Yet, a study from Jääskelainen et al. (2003) has observed that the concentration of cereulide inducing serious emetic food poisoning was approximately 1.6 μg of cereulide per gram of food, more than ten thousand times higher than the LoQ and level used for t_{cer} estimation in this study (0.02 ng per gram of matrix).

These findings suggest that the current guidelines based exclusively on *B. cereus* counts are adequate to ensure emetic toxin formation does not exceed critical levels, especially considering that natural contamination is generally lower than the inoculum level used in the present study (2–2.5 $\log_{10}$ CFU/mL). As reported by Shaheen et al. (2006), the total amount of cereulide produced in a fixed time interval increased with the increase on the quantity of inoculated bacteria. However, t_{cer} could also be used, where appropriate equipment and technique are available to measure cereulide, particularly when evaluating whether the current guidelines based on logcounts would guarantee non-detectable levels of toxin for different matrices.

Temperature abuse of food may occur in daily life. Considering the experimental set-up presented by this study, if DWM is left at 20 °C for 40 h, *B. cereus* counts reach the threshold level of 5 $\log_{10}$ CFU/mL and start forming cereulide if producer strains were present. Even if the product goes through a subsequent heat treatment to inactivate the bacteria, the toxin will not be destroyed.

When evaluating *B. cereus* growth and cereulide production in different food matrices, Ellouze et al. (2021) have reported that the matrix supporting the fastest growth will not necessarily allow the fastest cereulide production. The variability and uncertainty linked to cereulide production can make toxin production less predictable and matrix extrapolations limited, as shown by the validation study.

The scope of the present work was limited to five closely related dairy products, meaning that for a full risk assessment on the hazards connected to the emetic toxin production in dairy products additional data will be needed. However, the results presented in this study signifies one important step towards understanding how the emetic toxin is produced in such matrices to be able to predict it accurately and act preventively.

Declaration of competing interest

The authors have no competing interests to declare.

Acknowledgments

Marcel Tempelaars, Marie-Claude Courtet-Compondu and Christophe Fuerer are warmly acknowledged for their help with optimizing the LCMS/MS method and Mounia Bijlaart for her support with the experiments.

Funding

The authors declare that this study received funding from Nestlé. The study design, collection, analysis, interpretation of data and the conclusions of study are those of the authors.

Appendix A. Supplementary data

Supplementary data to this article can be found online at https://doi.org/10.1016/j.ijfoodmicro.2021.109519.

References

Agata, N., Mori, M., Ohta, M., Suwan, S., Ohtani, I., Isobe, M., 1994. A novel dodecadepsipeptide, cereulide, isolated from Bacillus cereus causes vacuole formation in HEp-2 cells. FEMS Microbiol. Lett. 121, 31–34.

Agata, N., Ohta, M., Yokoyama, K., 2002. Production of Bacillus cereus emetic toxin (cereulide) in various foods. Int. J. Food Microbiol. 73 (1), 23–27.

Andersson, M.A., Jääskeläinen, E.J., Shaheen, R., Pirhonen, T., Wijnands, L.M., Salkinoja-Salonen, M.S., 2004. Sperm bioassay for rapid detection of cereulide-producing *Bacillus cereus* in food and related environments. Int. J. Food Microbiol. 94, 175–183.

Andersson, A., Rönner, U., Granum, P.E., 1995. What problems does the food industry have with the spore-forming pathogens Bacillus cereus and Clostridium perfringens? Int. J. Food Microbiol. 28, 145–155.

Apetroaie-Constantin, C., Shaheen, R., Andrup, L., Smidt, L., Rita, H., Salkinoja-Salonen, M., 2008. Environment driven cereulide production by emetic strains of Bacillus cereus. Int. J. Food Microbiol. 127, 60–67.

Baranyi, J., Roberts, T.A., 1994. A dynamic approach to predicting bacterial growth in food. Int. J. Food Microbiol. 23, 277–280.

Bartoszewicz, M., Hansen, B.M., Swiecicka, I., 2008. The members of the Bacillus cereus group are commonly present contaminants of fresh and heat-treated milk. Food Microbiol. 25 (4), 588–596.

Buchanan, R.L., Whiting, R.C., Damert, W.C., 1997. When is simple good enough: a comparison of the gompertz, baranyi, and three-phase linear models for fitting bacterial growth curves. Food Microbiol. 14, 313–326.

Bursová, S., Necidová, L., Haruštiaková, D., 2018. Growth and toxin production of Bacillus cereus strains in reconstituted initial infant milk formula. Food Control 93, 334–343.
Carlin, F., Albagnac, C., Rida, A., Guinebretière, M., Couvert, O., Nguyen-The, C., 2013. Variation of cardinal growth parameters and growth limits according to phylogenetic affiliation in the Bacillus cereus Group. Consequences for risk assessment. Food Microbiology 33, 69–76.
Ceuppens, S., Rajkovic, A., Heyndrickx, M., Tsilia, V., Van De Wiele, T., Boon, N., Uyttendaele, M., 2011. Regulation of toxin production by Bacillus cereus and its food safety implications. Crit. Rev. Microbiol. 37, 188–213.
Delbrassinne, L., Andjelkovic, M., Rajkovic, A., Bottledoorn, N., Mahillon, J., Van Loco, J., 2011. Follow-up of the Bacillus cereus emetic toxin production in penne pasta under household conditions using liquid chromatography coupled with mass spectrometry. Food Microbiol. 28, 1105–1109.
Efsa, 2005. Opinion of the scientific panel on biological hazards (BIOHAZ) on Bacillus cereus and other Bacillus spp. in foodstuffs. EFSA J. 175, 1–48.
Efsa, 2016. EU summary report on zoonoses, zoonotic agents and food-borne outbreaks 2015. EFSA J. 14 (12), 4634.
Ehling-Schulz, M., Fricker, M., Grallert, H., Rieck, P., Wagner, M., Scherer, S., 2006. Cereulide synthetase gene cluster from emetic Bacillus cereus: structure and location on a mega virulence plasmid related to bacillus anthracis toxin plasmid pXO1. BMC Microbiol. 6, 20.
Ellouze, M., Buss da Silva, N., Rouzeau-Szynalski, K., Coisne, L., Cantergiani, F., Baranyi, J., 2021. Modeling Bacillus cereus growth and cereulide formation in cereal-, dairy-, meat-, vegetable-based food and culture medium. Front. Microbiol. 12, 639546.
Eneroth, A., Svensson, B., Molin, G., Christiansson, A., 2001. Contamination of pasteurized milk by Bacillus cereus in the filling machine. J. Dairy Res. 68, 189–196.
Finlay, W.J.J., Logan, N.A., Sutherland, A.D., 1999. Semiautomated metabolic staining assay for *Bacillus cereus* emetic toxin. Appl. Environ. Microbiol. 65, 1811–1812.
Finlay, W.J.J., Logan, N.A., Sutherland, A., 2000. Bacillus cereus produces most emetic toxin at lower temperatures. Lett. Appl. Microbiol. 31, 385–389.
Guerin, A., Rønning, H.T., Dargaignaratz, C., Clavel, T., Broussolle, V., Mahillon, J., Granum, P.E., Nguyen-The, C., 2017. Cereulide production by *Bacillus weihenstephanensis* strains during growth at different pH values and temperatures. Food Microbiol. 65, 130–135.
Guinebretière, M., Thompson, F.L., Sorokin, A., Normand, P., Dawyndt, P., Ehling-Schulz, M., Svensson, B., Sanchis, V., Nguyen-The, C., Heyndrickx, M., De Vos, P., 2008. Ecological diversification in the Bacillus cereus group. Environ. Microbiol. 10 (4), 851–865.
Guo, H., Yu, P., Yu, S., Wang, J., Zhang, J., Zhang, Y., Liao, X., Wu, S., Ye, Q., Yang, X., Lei, T., Zeng, H., Pang, R., Yhang, J., Wu, Q., Ding, Y., 2021. Incidence, toxin gene profiling, antimicrobial susceptibility, and genetic diversity of Bacillus cereus isolated from quick-frozen food in China. LWT 140, 110824.
Häggblom, M.M., Apetroaie, C., Andersson, M.A., Salkinoja-Salonen, M.S., 2002. Quantitative analysis of cereulide, the emetic toxin of Bacillus cereus, produced under various conditions. Appl. Environ. Microbiol. 68, 2479–2483.
Hornung, R.W., Reed, L.D., 1990. Estimation of average concentration in the presence of nondetectable values. Appl. Occup. Environ. Hyg. 5 (1), 6.
Huang, Y., Flint, S.H., Yu, S., Ding, Y., Palmer, J.S., 2021. Phenotypic properties and genotyping analysis of Bacillus cereus group isolates from dairy and potato products. In: LWT – Food Science and Technology 140:110853.
Jääskelainen, E.L., Teplova, V., Andersson, M.A., Andersson, L.C., Tammela, P., Andersson, M.C., Pirhonen, T.I., Saris, N.-E.L., Vuorela, P., Salkinoja-Salonen, M.S., 2003. In vitro assay for human toxicity of cereulide, the emetic mitochondrial toxin produced by food poisoning Bacillus cereus. Toxicol. in Vitro 17, 737–744.
Jääskeläinen, E.L., Häggblom, M.M., Andersson, M.A., Salkinoja-Salonen, M.S., 2004. Atmospheric oxygen and other conditions affecting the production of cereulide by Bacillus cereus in food. Int. J. Food Microbiol. 96, 75–83.
McAuley, C.M., McMillan, K., Moore, S.C., Fegan, N., Fox, E.M., 2014. Prevalence and characterization of foodborne pathogens from australian dairy farm environments. J. Dairy Sci. 97, 7402–7412.
Oliveira Silva, H., Santos Lima, J.A., Aguilar, C.E.G., Rossi, G.A.M., Mathias, L.A., Vidal, A.M.C., 2018. Efficiency of different disinfectants on Bacillus cereus sensu stricto biofilms on stainless-steel surfaces in contact with milk. Front. Microbiol. 9, 2934.
Park, K.M., Kim, H.J., Jeong, M., Koo, M., 2020. Enterotoxin genes, antibiotic susceptibility, and biofilm formation of low-temperature-tolerant Bacillus cereus isolated from green leaf lettuce in the cold chain. Foods. 9, 249.
Rajkovic, A., Uyttendaele, M., Ombregt, S., Jaaskelainen, E., Salkinoja-Salonen, M., Debevere, J., 2006. Influence of type of food on the kinetics and overall production of Bacillus cereus emetic toxin. J. Food Prot. 69, 847–852.
Ratkowsky, D.A., Olley, J., McMeekin, T.A., Ball, A., 1982. Relationship between temperature and growth rate of bacterial cultures. J. Bacteriol. 149, 1–5.
Shaheen, R., Andersson, M.A., Apetroaie, C., Schulz, A., Ehling-Schulz, M., Ollilainen, V., Salkinoja-Salonen, M.S., 2006. Potential of selected infant food formulas for production of Bacillus cereus emetic toxin, cereulide. Int. J. Food Microbiol. 107, 287–294.
Shinagawa, K., Ueno, Y., Hu, D., Ueda, S., Sugii, S., 1996. Mouse lethal activity of a HEp-2 vacuolation factor, cereulide, produced by Bacillus cereus isolated from vomiting-type food poisoning. J. Vet. Med. Sci. 58, 1027–1029.
Svensson, B., Ekelund, K., Ogura, H., Christiansson, A., 2004. Characterisation of Bacillus cereus isolated from milk silo tanks at eight different diary plants. Int.< span/>DairyJ. 14 (1), 17–27.
Svensson, B., Monthán, A., Shaheen, R., Andersson, M.A., Salkinoja-Salonen, M., Christiansson, A., 2006. Occurrence of emetic toxin producing Bacillus cereus in the dairy production chain. Int. Dairy J. 16 (7), 740–749.
Szabo, R.A., Speirs, J.I., Akhtar, M., 1991. Cell culture detection and conditions for production of a Bacillus cereus heat-stable toxin. J. Food Prot. 54, 272–276.
Walser, V., Kranzler, M., Dawid, C., Ehling-Schulz, M., Stark, T.D., Hofmann, T.F., 2021. Distribution of the emetic toxin cereulide in cow milk. Toxins. 13, 528.
Wijnands, L.M., Dufrenne, J.B., Rombouts, F.M., van Leusden, F.M., in't Veld, P.H., 2006. Prevalence of potentially pathogenic Bacillus cereus in food commodities in The Netherlands. Journal of Food Protection 69, 2587–2594.